

## Soft ionic-hydrogel electrodes for electroencephalography signal recording

SHENG XinJun<sup>1,2\*</sup>, QIN Zhun<sup>1</sup>, XU HaiPeng<sup>1</sup>, SHU XiaoKang<sup>1</sup>, GU GuoYing<sup>1,2</sup> & ZHU XiangYang<sup>1,2</sup>

<sup>1</sup> Robotics Institute, School of Mechanical Engineering, Shanghai Jiao Tong University, Shanghai 200240, China;

<sup>2</sup> State Key Laboratory of Mechanical System and Vibration, Shanghai Jiao Tong University, Shanghai 200240, China

Received March 31, 2020; accepted May 18, 2020; published online September 10, 2020

Wet gel electrodes have been widely used for electroencephalography (EEG) signal recording, which generally causes skin abrasion and longer preparation time. In this paper, we present soft ionic-hydrogel based electrodes to overcome such drawbacks. In order to conveniently measure the EEG signals, we design the claw-like and patch-like structures for robust connection between metal (Ag/AgCl) electrodes and skin scalps. Next, we experimentally show that the soft ionic-hydrogel based electrodes have similar performance with the conventional wet gel electrodes in terms of the short-circuit noise, electrical impedance, and skin-electrode contact impedance on unprepared human skin, significantly better than dry electrodes and water-based electrodes. We further perform the EEG measurements and steady-state visual evoked potentials (SSVEP) experiments with five subjects to verify the effectiveness of the soft ionic-hydrogel based electrodes. The experimental results demonstrate that our developed soft ionic-hydrogel electrodes can record high-quality EEG signals in a fast and clean way, being a compelling option for EEG-based brain-computer interfaces.

**brain-computer interface, EEG, electrodes, ionic hydrogel, soft materials**

**Citation:** Sheng X J, Qin Z, Xu H P, et al. Soft ionic-hydrogel electrodes for electroencephalography signal recording. *Sci China Tech Sci*, 2020, 63, <https://doi.org/10.1007/s11431-020-1644-6>

### 1 Introduction

Brain-computer interfaces (BCI) enable direct communication between human brain and external devices using cortical activities as the control signal. As a noninvasive measurement of electrical cortical activities, electroencephalography (EEG) provides highly resolved temporal information to reflect the dynamics of brain activities [1]. It has been widely used in BCI researches [2–6] due to its convenience, high mobility, easy setup, and relatively low cost [7]. In order to acquire high-quality EEG signals, conventional Ag/AgCl electrodes are generally used with wet conductive gel to guarantee low skin-electrode impedance (<5 K $\Omega$ ). However,

the application of conventional gel electrodes is usually time-consuming for electrode preparation and washing the cap at each electrode site after the experiment [8]. Besides, the conductive gel inevitably leaves residues, which makes the hair dirty and brings remarkable inconvenience to the users. Another inconvenience for users is that they need to inject conductive gel carefully at each electrode site to reduce skin-electrode impedance and avoid the short circuit caused by flowability of the conductive gel [9], which requires some specialized training. Moreover, the recording time is limited due to the drying effects of the conductive gel [10].

In order to overcome the above limitations of gel electrodes, many kinds of new electrodes have been developed. One of them is the dry electrode, such as pin-shaped metal

\*Corresponding author (email: [xjsheng@sjtu.edu.cn](mailto:xjsheng@sjtu.edu.cn))

electrodes [11] or soft conductive polymer electrodes [12]. However, the skin-electrode impedance of dry electrodes is high, and the friction between scalps and electrode pins brings motion artifacts. To reduce the skin-electrode impedance, water-based electrodes [13] and bristle-shaped semi-dry electrodes are proposed [14]. The utilization of pure water or saline solution for conduction leaves few residues on hair and achieves lower contact impedance than dry electrodes. The disadvantage of using the conductive fluid is the high evaporation rate, which increases the contact impedance dramatically over time. On the other hand, it may create short circuits between adjacent electrodes easily [15].

With the development of flexible electronics, many stretchable electrodes with flexible functional materials are developed [16,17]. Ionic hydrogels, which contain conductive salts, are emerging rapidly as a new class of transparent flexible material [18]. As a soft ionic conductor, the hydrogel has good conductivity, low interfacial impedance, and strong wetting effects to the skin surface [19]. Currently, several hydrogels have been explored for EEG signals recording, for instance, cross-linked sodium polyacrylate gel swelled with electrolyte [20], AG602 hydrogel membrane [21] and polyacrylamide (PAAM) hydrogel [22]. These hydrogels are generally attached to human skin directly and function as the conductive medium. Because these hydrogels are too soft to penetrate through the hair, they can only be used on the scalps without hair. To solve the problem, Pedrosa et al. [23] design an alginate-based hydrogel. This hydrogel can be injected on the scalp as a viscous liquid, and forms a solid hydrogel in a few minutes, ensuring faster cleaning procedures. But it inevitably brings much pain when the alginate-based hydrogel is removed from user's hair. Due to the rapid gelation rate, users need to prepare more than one hydrogel batch in one experiment if many electrode sites are required. To the best of our knowledge, no existing hydrogel electrodes can be conveniently utilized to acquire high-quality EEG signals on the hairy scalps.

In this paper, we present soft ionic-hydrogel based electrodes for EEG signal recording. The ionic hydrogel is designed to contact metal (Ag/AgCl) electrodes and skin scalps replacing conventional conductive gel. Because the hydrogel is a soft solid material, there is no residue left on the scalp after the experiment. In order to achieve low skin-electrode contact impedance, claw-like and patch-like electrode structures assembled by 3D printed components are designed. At hairy sites, the claw-like electrode structure is designed to penetrate the hair. The cylindrical hydrogel is put in the electrode container and extruded to form hemispherical protruding structures at the end of the five claws to contact the scalp. At the forehead without hair, the cylindrical hydrogel is sectioned into small slices and attached to the Ag/AgCl electrode directly. The cylindrical hydrogel can be mass produced and stored for about 18 days for con-

venient usage. Compared with other electrodes based on hydrogel, the main advantage of our design is that unique electrode structures ensure comfortable and good skin-electrode contact, and it can be prepared and stored conveniently for practical use. To evaluate the performances of the ionic-hydrogel electrodes, commercial gel electrodes, dry electrodes, and water-based electrodes are employed for comparison. The ionic-hydrogel electrodes show good noise levels and high electrical performance. It dramatically reduces skin-electrode impedance due to wetting effects and a larger area of contact surface. The EEG signal measurements and steady-state visual evoked potentials (SSVEP) experiments with five subjects show that our new electrodes are comparable with conventional gel electrodes, even on the hairy scalp.

## 2 Materials and methods

### 2.1 Design of the ionic-hydrogel electrodes

#### 2.1.1 Ionic hydrogel synthesis

The ionic hydrogel is the polyacrylamide (PAAm) hydrogel containing NaCl and synthesized referring to a previously published method [24]. The precursor ink of PAAm-NaCl hydrogel is synthesized by mixing the acrylamide (AAM; J&K) monomer solution, *N,N'*-methylenebisacrylamide (MBAA; Molbase) crosslinker solution and 2-Ketoglutaric acid (Adamas) photoinitiator with the mass ratio of 96.67%:1.13%:2.20%. The monomer solution is prepared by mixing AAM, NaCl and deionized water with a mass ratio of 9.98%:16.16%:73.86%. The MBAA solution is prepared by mixing MBAA into deionized water with a mass ratio of 1.2%. The solution is agitated with a magnetic stirrer for 1 h to form a homogeneous solution. Here, NaCl is chosen as the conductive medium due to its good biocompatibility.

To fabricate the cylindrical ionic hydrogel, the molding method is then utilized. The ionic-hydrogel precursor ink is injected into the cylindrical mold through a needle. Afterward, the ultraviolet light with the power of 500 W and the wavelength of 365 nm is applied to initiate the crosslinking for about 30 min. After the crosslinking process, the cured hydrogel is removed from the mold.

#### 2.1.2 Electrode structures design

To penetrate through the hair and increase the hydrogel-skin contact area, claw-like electrodes are developed (Figure 1, weight 7.9 g). The electrode components are fabricated by a 3D printer (J750, Stratasys Co. Ltd., USA), and the claws are printed with a kind of rubber-like material (Agilus30, Stratasys Co. Ltd., USA). The cylindrical hydrogel is 10 mm height and 12 mm in diameter, which fits into the container. Each cylindrical hydrogel costs about \$0.01. Five holes with a diameter of 3 mm are placed at the bottom of the container

in a circular array. The claws are hollow and stretch out at an angle of  $30^\circ$  from the axis. The length of the claws is 6 mm. Five claws ensure stable placement of the electrodes on human scalps and a large contact area. The Ag/AgCl electrode ( $d=8$  mm,  $h=1$  mm) is fixed by hot melt glue and 0.2 mm protruding for better contact with the hydrogel. To prevent hydrogel distortion when twisting the thread, the key-slot structure is designed to ensure that the cylinder push rod can only do a linear movement. The screw shell is thus designed to rotate relatively to the push rod.

When preparing the electrode, users need to put the hydrogel into the container and extrude the hydrogel with the screw to drive it exposed from the claws (Figure 2(a)). A hemispherical protruding structure will be formed at the end of the claws (Figure 2(b)). The electrode can contact the scalp with these hydrogel hemispheres. To reduce the skin-electrode contact impedance and prevent hydrogels from breaking, we use the screw to squeeze out the hydrogel 4–5 mm height. The skin-hydrogel contact area reaches about  $75$  mm<sup>2</sup> when the contact is stable. For electrodes on the forehead, the hydrogels are sectioned with surgical

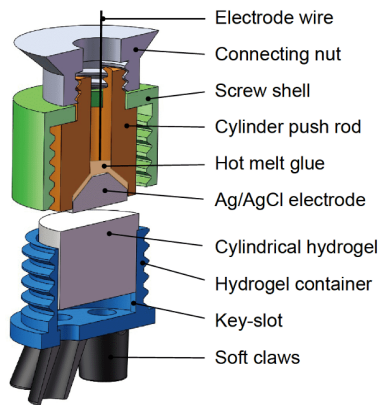


**Figure 1** The cutaway view of the claw-like ionic-hydrogel electrode.

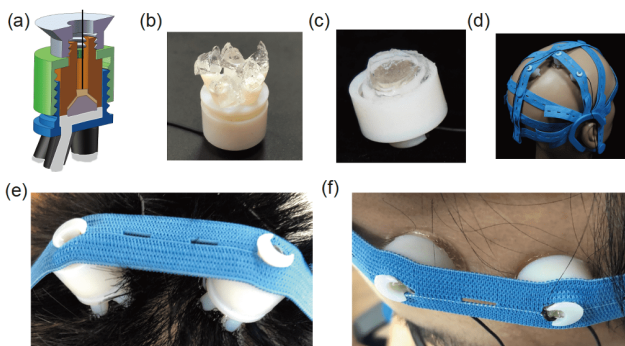


**Figure 2** Preparation process of soft ionic-hydrogel electrodes. (a) The assembled claw-like electrode model for hairy scalps; (b) the assembled claw-like electrode product for hairy sites; (c) the assembled patch-like electrode product for forehead without hair; (d) the EEG cap for electrode fixing; (e) the photo of the claw-like electrodes on hairy scalps; (f) the photo of the patch-like electrodes on the forehead without hair.

scissors into small slices, each approximately 3 mm thick and 12 mm in diameter. The slices are then attached to the Ag/AgCl electrode directly to form patch-like electrodes (Figure 2(c), weight 5.8 g). The skin-hydrogel contact area of the patch-like electrode is about  $150$  mm<sup>2</sup> when stable. A simple cap with small holes (Figure 2(d), weight 44.6 g) is used to fix the electrodes on human heads. For BCI applications with no more than 15 electrodes, the entire device weighs no more than 200 g and is very comfortable to wear. Enlarged views of ionic-hydrogel electrodes on hairy scalps and forehead are displayed in Figure 2(e) and (f), respectively. Figure 3 shows the flow chart for the preparation of PAAm-NaCl hydrogel and ionic-hydrogel electrodes.

## 2.2 Materials and apparatus for measurements

The performance of ionic-hydrogel electrodes is evaluated with controlled experiments. Gel electrodes (ECI Electro-Gel, Electro-Cap International Inc., OH, USA), dry electrodes (OpenBCI, <https://shop.openbci.com>) and water-based electrodes with a saline solution of 4.5 g NaCl/150 mL water (Greentek, Wuhan Greentek Pty. Ltd., China) are introduced for comparison. A SynAmps2 system (Neuroscan, USA) is used for EEG signal measurements and the electrodes are distributed according to the extended international 10–20 systems. The reference electrode is located on the vertex, and the ground electrode is located on the forehead. The sampling rate is set to 1000 Hz, and an analog filter with a frequency band of 0.5–200 Hz is applied. All the electrodes are carefully adjusted to achieve well skin-electrode contacts. All subjects in the study are recruited from Shanghai Jiao Tong University. The experiments in this study are designed following the declaration of Helsinki.

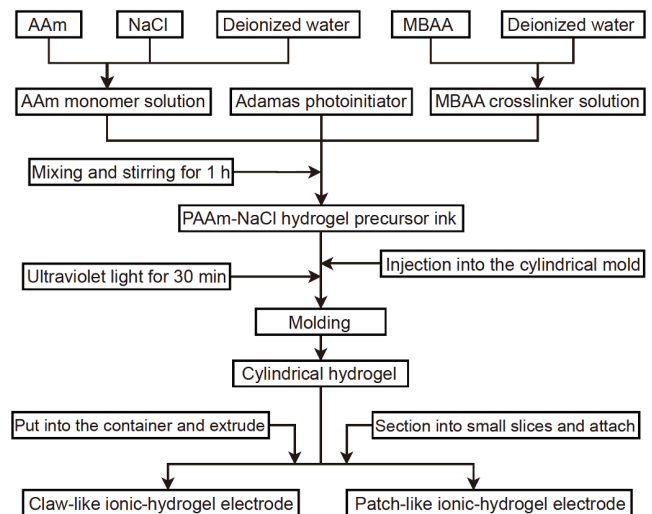


**Figure 3** Flow chart for the preparation of PAAm-NaCl hydrogel and ionic-hydrogel electrodes.

### 3 Results

#### 3.1 Measurements in short circuit

The performance of the ionic-hydrogel electrodes is firstly compared with gel electrodes, dry electrodes, and water-based electrodes in the short circuit. The data of different kinds of electrodes is recorded and evaluated by collecting the signals between two same kinds of electrodes. The two same electrodes are attached to a polished copper plate (10 cm×10 cm) at a fixed distance of 5 cm.

##### 3.1.1 Short-circuit noise test

The potential difference between two electrodes in short circuit which is considered as noise [14] is tested with a multichannel amplifier (g. Hlamp, g.tec medical engineering GmbH, Austria). The short-circuit noise is recorded with a sampling rate of 256 Hz. Figure 4 shows the short-circuit noise of the different electrodes for 60 s. The short-circuit noise is band-pass filtered with a frequency band of 1–45 Hz, which is a typical frequency range for EEG-based BCI applications. SynAmps2 is not used here because SynAmps2 must be configured for at least three electrodes (GND, reference, and signal channel).

The amplitudes of short-circuit noise in Figure 4(d) show that dry electrodes achieve the least and the most stable noise level. The results in Figure 4(b) and (c) show that ionic-hydrogel electrodes with or without claws have similar noise levels with gel electrodes (Figure 4(a)), which may benefit

from ionic hydrogel's flexibility and good conductivity. The water-based electrode in Figure 4(e) shows the maximum noise. Figure 4(g) and (h) show the number of noise signals at different amplitudes recorded by ionic-hydrogel electrodes. The normal distribution of short-circuit noise conforms to the random Gaussian noise and can be eliminated by some signal processing methods, such as wavelet denoising [25], indicating that ionic-hydrogel electrodes are less disturbed. Besides, ionic-hydrogel electrodes have less noise power than gel electrodes (Figure 4(f)) because the noise is more concentrated near 0  $\mu\text{V}$ . Figure 4(i) and (j) show the number of noise signal at different amplitudes recorded by dry electrodes and water-based electrodes, respectively.

##### 3.1.2 Short-circuit impedance test

The impedance values of the ionic-hydrogel electrodes in short circuit are then measured by a Keysight E4980AL LCR meter at 30 Hz, 5 mV root mean square (RMS) value. Impedance values are calculated to be half of the impedance tested between electrodes, ignoring the impedance of copper plate. Figure 5 illustrates the results of a 2-h study comparing impedance values in the short circuit, tested at an interval of 10 s. Patch-like ionic-hydrogel electrodes have a little higher impedance than gel electrodes, but the impedance decreases over time, presumably due to a slower skin wetting effect of ionic hydrogels than conductive gels. Claw-like ionic-hydrogel electrodes have a trend toward increasing the impedance and its variation because of a smaller and unstable

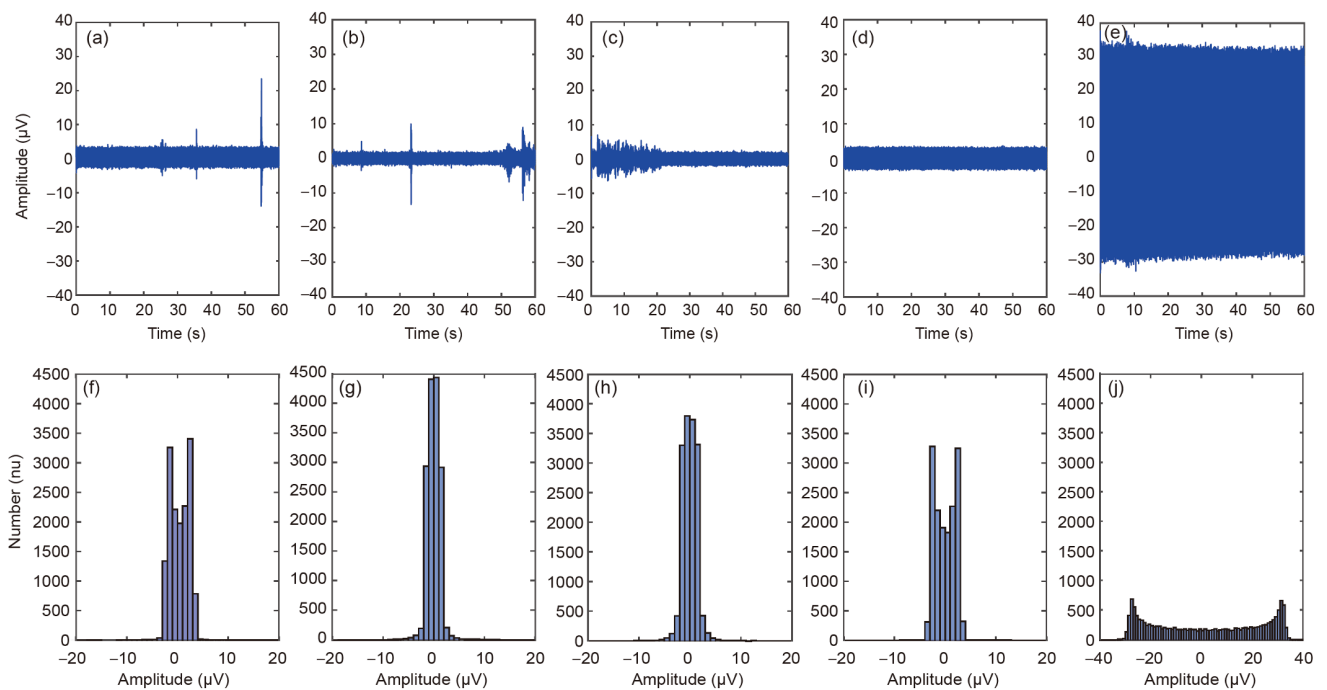


**Figure 4** (Color online) Short-circuit noise test. Noise measured by commercial gel electrodes (a), patch-like ionic-hydrogel electrodes (b), claw-like ionic-hydrogel electrodes (c), dry electrodes (d) and water-based electrodes (e). The number of noises at different amplitudes by commercial gel electrodes (f), patch-like ionic-hydrogel electrodes (g), claw-like ionic-hydrogel electrodes (h), dry electrodes (i) and water-based electrodes (j).



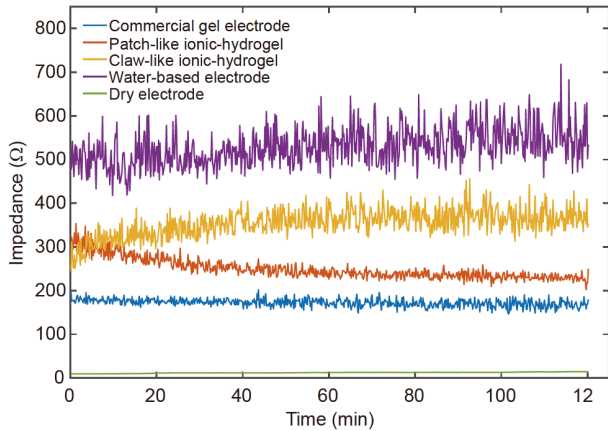


**Figure 5** Comparison of the impedance in short circuit for the typical individual electrode of five different types, measured at 30 Hz, 5 mV RMS.

contact area of the claws with the copper plate, but still lower than water-based electrodes. As good conductors, dry electrodes have low impedance ( $<10 \Omega$ ).

### 3.2 Skin-electrode contact impedance test

In order to assess the interfacial performance of the ionic-hydrogel electrodes on human skin, the forehead and hairy sites are selected to test skin-electrode contact impedance. Contact impedances are collected from three human subjects at two different positions (F10, Fp1) on the forehead and three different positions (Fz, P3, P6) on hairy sites. For each scalp position, two same kinds of electrodes are placed respectively (approximately 3 cm apart). The contact impedance is also measured by E4980AL. Each position is tested for 20 times. Electrodes are positioned in an alternating fashion to assure varying locations for each electrode. The forehead skin for test is gently washed with water and patted dry to assure that all subjects presented normal skin surface conditions. After 5 min of contact for electrode stabilization, the impedance between electrodes is measured. Because the contact impedance is measured with a reference electrode, the actual impedance is reported as half of the measurement results [26].

Figure 6 shows the averaged impedance values of different electrodes on the forehead. The frequency of test signal for forehead is ranged from 20 to 1000 Hz to provide a broad frequency impedance comparison. The result shows that the ionic-hydrogel electrode has smaller contact impedance than the gel electrode and water-based electrode. The ionic-hydrogel electrode achieves the smallest standard deviation which represents the stability and consistency of skin-electrode contact.

Table 1 shows the contact impedance of different electrodes on the hairy sites for the three subjects. The frequency of the test signal for hairy sites is fixed to 30 Hz, which is

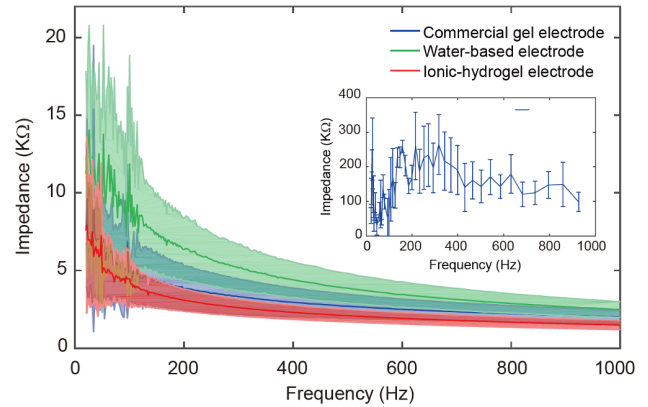


**Figure 6** Skin-electrode contact impedance of different electrodes at different frequencies on the forehead without hair (F10, Fp1).

**Table 1** Impedance (KΩ) on hairy sites of different electrodes ( $N=60$ )

Electrode	Subject			
	S1	S2	S3	Average
Gel	6.2±2.3	4.3±1.8	2.2±0.3	4.2
Ionic-hydrogel	22.1±3.9	25.6±2.5	4.6±0.9	17.4
Water-based	23.0±3.7	28.8±6.8	4.1±0.9	18.7
Dry	120.9±56.6	202.2±51.8	94.4±49.1	139.1

consistent with commercial EEG device SynAmps2 [27]. Commercial gel electrodes show the smallest impedance as expected, which arises from the excellent flowability of gel. After careful preparation, the impedance values can be reduced below 5 KΩ. Water-based electrodes show higher impedance values than gel electrodes, mainly because sponge cannot be well adapted to scalps across the hair. The contact impedance performance of ionic-hydrogel electrodes is far better than dry electrodes, similar to the water-based electrodes. However, ionic-hydrogel electrodes avoid drawbacks of water-based electrodes that have strong drying effects and are accessible to short circuit.

### 3.3 Comparison of EEG signals quality

EEG signals are collected and compared between gel electrodes and ionic-hydrogel electrodes. Figure 7 shows a section of 5 s long EEG signals at Fp1 and Fp2 from the patch-like ionic-hydrogel electrode and gel electrode, respectively. Two similar eye blinking potentials are simultaneously observed from both electrodes. Figure 8 shows envelopes of alpha oscillations when the subjects are instructed to open or close their eyes [28]. The claw-like ionic-hydrogel electrode and gel electrode are placed carefully in adjacent positions at the occipital region. The envelopes are computed using the Hilbert transform implemented in MATLAB for a clear observation. The spectrum of EEG signals measured by gel and ionic-hydrogel electrodes shows a similar change tendency.

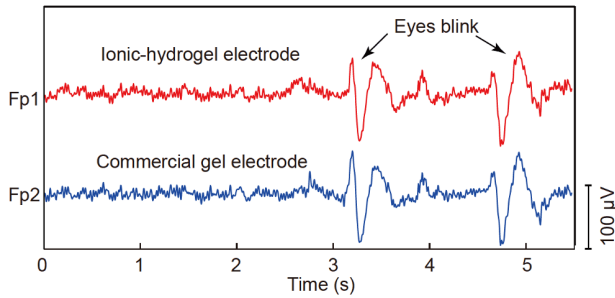


**Figure 7** EEG signals recording (5 s) by ionic-hydrogel and commercial gel electrodes.

Afterwards, the signal quality of the gel and ionic-hydrogel electrodes is furtherly investigated. The ionic-hydrogel electrode is placed close to the gel electrode with a distance of 15 mm to avoid short circuit. 5 s EEG signals are simultaneously collected from both electrodes. **Figure 9** shows the electrode placements and results of raw EEG signals measured at the forehead (F10) and hairy sites (Pz), respectively. The correlation coefficient between EEG signals from paired electrodes is more than 0.9 (0.9365 at the forehead and 0.9564 at hairy sites). It demonstrates the EEG signals quality of the ionic-hydrogel electrode is really close to that of gel electrode.

### 3.4 SSVEP user-centered test

SSVEP experiments are carried out to evaluate the effectiveness and efficiency of ionic-hydrogel electrodes for BCI applications. An LED monitor (Samsung S22B150, 1920×1080 pixel screen resolution) is used as a stimulator. The monitor's refresh rate is set to be 50 Hz. **Figure 10(a)** shows the distribution of the four targets on the screen, which are flashing at 7.14, 8.33, 10, and 12.5 Hz respectively. The

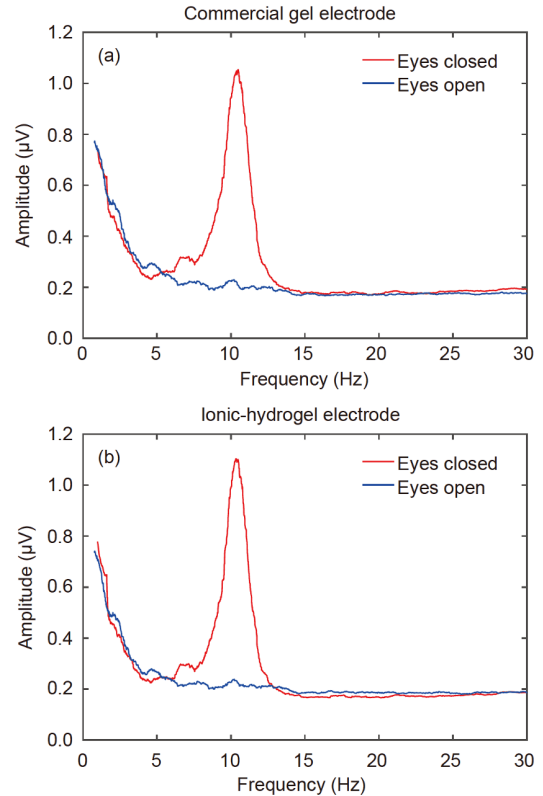


**Figure 8** Results of the EEG recording in eyes open/closed paradigm for 60 s from a representative subject. The spectra of gel electrode (a) and ionic-hydrogel electrode (b) are acquired from adjacent positions at the occipital region.

checkerboard pattern consists of 5×5 arrayed squares with a size of 8 cm (W)×8 cm (L). Black squares are flipped to white squares and white squares to black squares for each flickering. An arrow appears randomly and points to one of the four targets, representing where the flickering block will

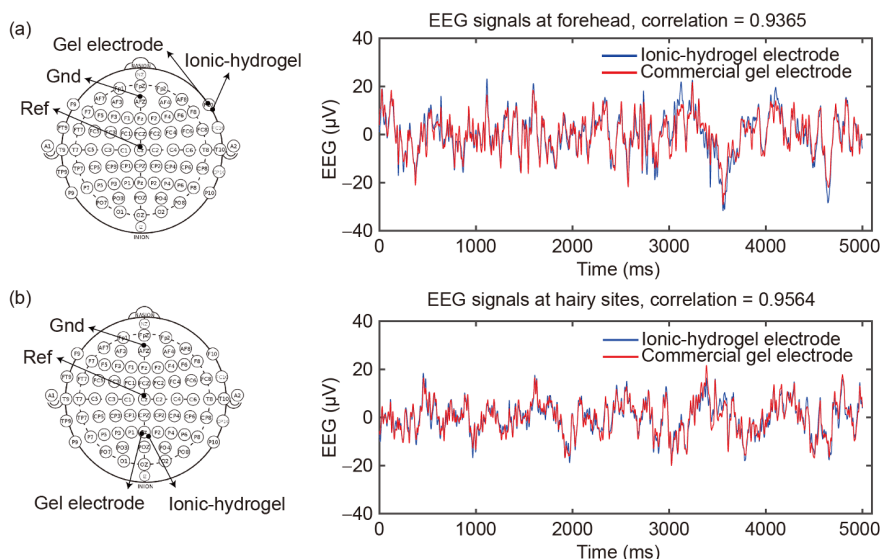


**Figure 9** Electrode placements and results of EEG signals recorded on the forehead (F10) (a) and EEG signals recorded on hairy sites (Pz) (b).

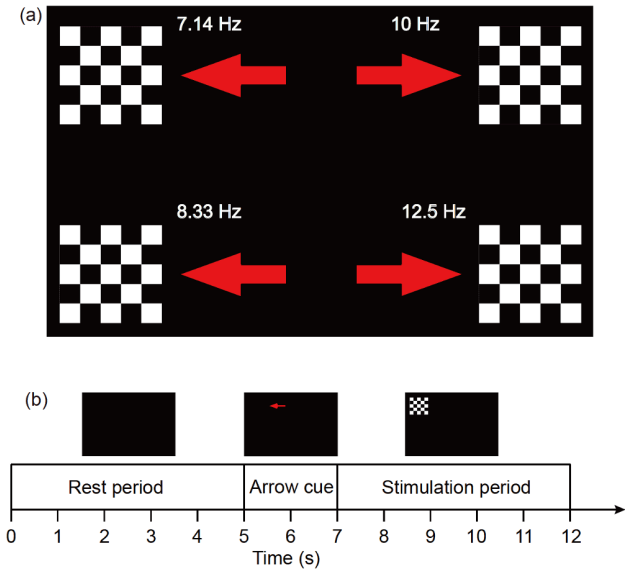


**Figure 10** Experimental paradigm description of SSVEP. (a) The distribution of four checkerboard targets on the monitor; (b) timing scheme of a single trial.

appear and subjects should gaze at.

Five healthy adults (S1–S5) with normal or corrected-to-normal vision participate in the experiment. The subjects' hair length is ranged from 3 to 8 cm. For each subject and each kind of electrodes, the experiment includes two blocks. Each block contains 40 trials (10 trials for each stimulation frequency), and there is a rest about 5 min between the two blocks. Each trial starts with a 5 s rest, and then a 2 s arrow appears. Subjects are next instructed to focus their eyes on the corresponding target for 5 s. Each trial lasts 12 s in total (Figure 10(b)). EEG signals from three channels at the occipital area (O1, Oz, O2) are simultaneously recorded for each experimental condition.

Figure 11(a) and (b) show the averaged frequency spectrum of the three positions (O1, Oz, O2) from a representative subject (S5). For higher signal-noise ratio (SNR), EEG segments of 20 trials for each stimulation type are spliced for spectrum analysis. For claw-like ionic-hydrogel electrodes, peaks at 7.14, 8.33, 10, 12.5 Hz, and their harmonics can be precisely and obviously recognized.

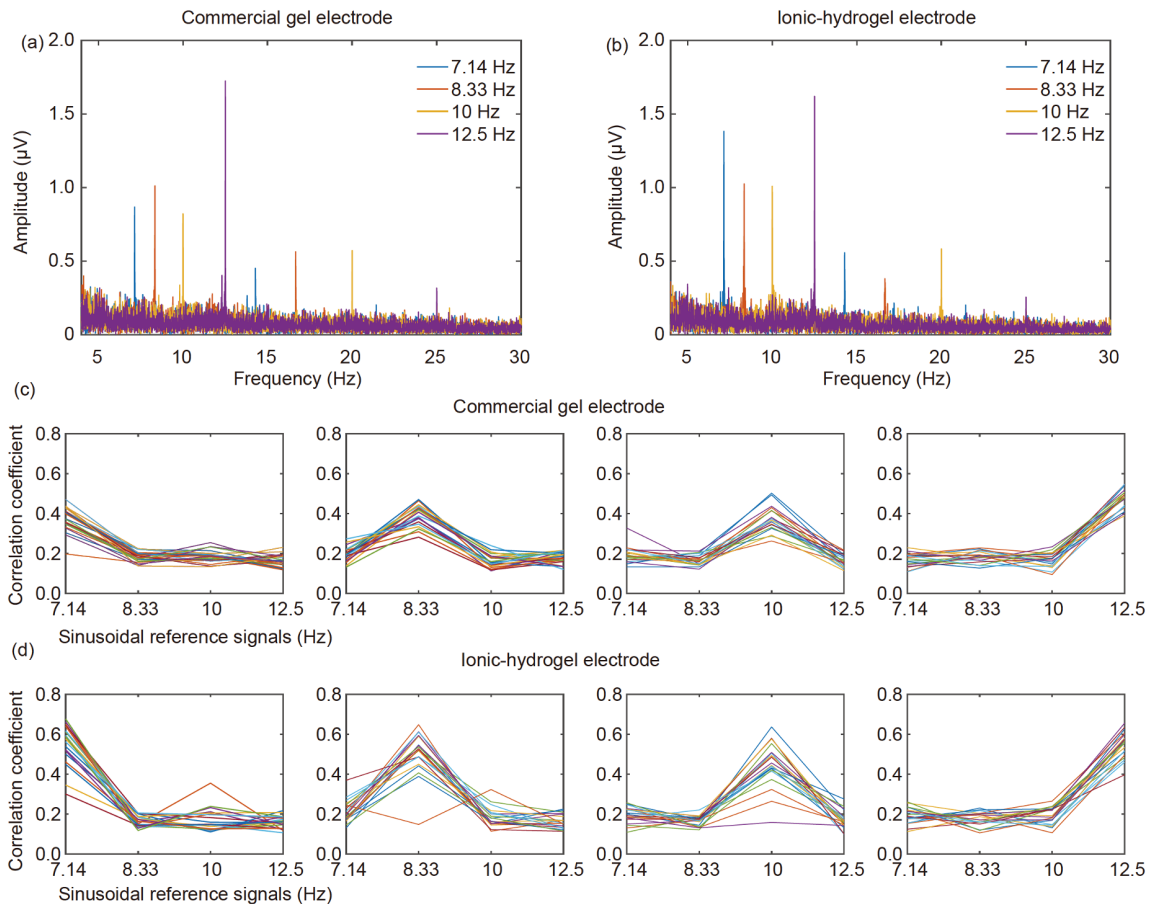


**Figure 11** SSVEP evaluations for gel and ionic-hydrogel electrodes from a representative subject (S5). The averaged frequency spectrum of EEG signals with different stimulation frequencies between three positions (O1, Oz, O2) for gel electrodes (a) and ionic-hydrogel electrodes (b). The CC values between the processed EEG signals and predefined sinusoidal reference signals calculated by CCA for gel electrodes (c) and ionic-hydrogel electrodes (d). The four figures from left to right correspond to the four results when different flashing frequencies (7.14, 8.33, 10, 12.5 Hz) are shown to the subject. The 20 colored lines in each figure correspond to the 20 trials.

**Table 2** Recognition accuracy of SSVEP across five subjects

Subject	Electrode	
	Gel electrode (%)	Ionic-hydrogel electrode (%)
S1	98.75	98.75
S2	100	97.5
S3	87.5	82.5
S4	100	95
S5	100	97.5
Average	97.25±5.48	94.25±6.71

Furthermore, the peak characteristic of the frequency-domain power spectrum between gel and ionic-hydrogel electrodes are very similar. Notably, the ionic-hydrogel electrodes show a higher response at the low-frequency flash (7.14 Hz).

To assess the recognition accuracy of SSVEP, the correlation coefficient (CC) values between predefined sinusoidal reference signals at stimulation frequencies and the corresponding multichannel EEG data are calculated in the frequency domain via a canonical correlation analysis (CCA) algorithm [29]. The result with the maximum CC value is identified as the target. Gel electrodes (Figure 11(c)) and ionic-hydrogel electrodes on hairy sites (Figure 11(d)) show similar outcomes among 80 trials of the SSVEP experiment for subject S5.

The BCI recognition accuracies across five subjects are shown in Table 2. For each subject and each kind of electrodes, 80 trials are extracted for BCI recognition. Segment [0.15 s, 5.15 s] of each trial is used for decoding in consideration of a user delay, where the time 0 indicates stimulus onset. All data epochs are firstly band-pass filtered between [6 Hz, 40 Hz] with Chebyshev type I infinite impulse response (IIR) filters. Then, the standard CCA process is applied to each EEG signal segment. The first three harmonics of all electrodes are used in the CCA algorithm. The averaged BCI accuracies of five subjects are 97.25% and 94.25% for gel and ionic-hydrogel electrodes, respectively. The accuracy gap is small enough for our proposed ionic-hydrogel electrodes to replace conventional gel electrodes.

### 3.5 Performance usability in the long term

To further demonstrate the potential of ionic-hydrogel electrodes for practical application, long-term skin-electrode contact impedance variations in a single day (3.5 h) and different days (18 d) are evaluated. Figure 12(a) shows the impedance measurement results (3.5 h) on the forehead and hairy sites, which are measured every 0.5 h. The impedance on hairy sites is ranged from 10 to 30 K $\Omega$ , and the impedance on forehead is below 10 K $\Omega$ . The impedances on both sites are acceptable for BCI experiments below 40 K $\Omega$  [30].

For cross-day measurements, a large number of hydrogels are produced at a time, and then four new hydrogel samples

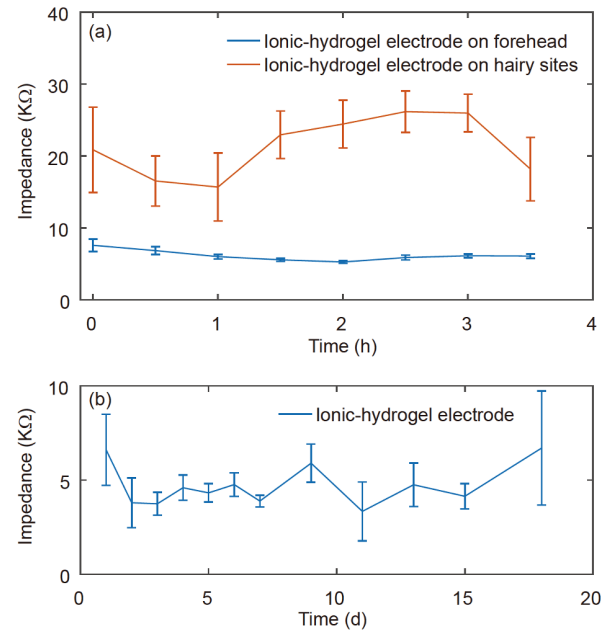


**Figure 12** Impedance variations of ionic-hydrogel electrodes for long-term usability. Results are measured at 30 Hz, 5 mV RMS. Impedance test for ionic-hydrogel electrodes on forehead and hairy sites in a single use for 3.5 h (a) and on forehead across different days (b).

are taken out from the storage box in a new day for assessment. We store the produced hydrogel in a moderate humidity environment. Specifically, we set up a sealed box with water depth of 3 mm. We put a platform in the box and put the hydrogel on the platform to avoid direct contact with water. Other conditions are not strictly required. Figure 12(b) shows the impedance variation of ionic-hydrogel electrodes across different days. Only the forehead is selected for evaluation due to easy accessibility and skin condition consistency. The assessment lasts for 18 d, and we find that skin-electrode contact impedance keeps below 10 K $\Omega$ . The results prove the stability and usability of our proposed ionic-hydrogel electrodes in the long-term application.

## 4 Discussion

In this work, soft ionic-hydrogel electrodes for EEG signal recording is proposed and evaluated as a convenient and clean monitoring method. Claw-like electrodes penetrate through the hair to provide low skin-electrode contact impedance. Hydrogel hemispheres from five claws increase the hydrogel-skin contact area, which lowers the intensity of pressure from the flexible cap. Besides, the claws are fabricated with a kind of rubber-like soft material. Because of the attentive design, all subjects feel no pain in experiments lasting up to 2–3.5 h. Additionally, users just need to put the hydrogel into the container and screw the thread when they prepare the electrode. This is a convenient process, which



requires little effort and takes no more than 20 s. Furthermore, the hydrogel can be mass produced at a low cost (each \$0.01) and stored for about 18 d. The separation of hydrogel production and electrode preparation makes the practical applications possible.

As soft materials, PAAm-NaCl ionic hydrogel shows good conductivity and flexibility. It permits better ionic conductivity by dissolved mobile ionic species, which is similar to electrolytic tissue media [31]. The noise introduced by hydrogel is as small as dry electrodes (Figure 4). EEG is non-stationary signals with amplitudes of several dozens of microvolts [32]. Less noise means higher SNR in EEG-based BCI. This small noise and low impedance (Figure 5) are owing to the functional good properties of hydrogel and multiple attempts of the different material ratio of the hydrogel. For dry electrodes, although as good conductors, skin-electrode contact impedance are usually over 100 K $\Omega$  [33]. It mainly arises from rigid metals pins, which cannot adapt to the scalp well, although pins penetrate hair easily. The high contact impedance of dry electrodes leads to undesired effects of mismatch impedance in differential EEG measurements, and thus a higher cost of EEG amplifiers with ultra-high impedance is needed. For ionic-hydrogel electrodes, softness and functional adaptability of hydrogel ensure comfort and good contact with skin (Figure 6). Even on the hairy sites, contact impedance can still reach a close level to the water-based electrodes, which infiltrates scalp with saline solution (Table 1). To be noticed, for subject S3 in Table 1, who has sparse hair, skin-electrode contact impedance of ionic-hydrogel electrodes reaches below 5 K $\Omega$ , which is similar to the contact impedance after conductive gel application. Besides, the hydrogel shows good wetting effects as a hydrate. Its high contents of water reduce contact impedance furtherly and rapidly. These excellent physical properties of hydrogel ensure high-quality EEG signals and effective BCI performance.

Previous studies focusing on hydrogel for EEG recording consider little about its storage, user convenience, and long-term usability [20,23]. However, this matters a lot in practical use. As a hydrate, ionic hydrogel dehydrates quickly. If hydrogel has to be remade before each use, the application will be impossible outside the laboratory without raw materials and professional equipment. In this work, we explore two simple methods for hydrogel storage and use. One method is that we expose the hydrogel to the air at room temperature without any protection. The hydrogel will dehydrate and dry over time. Each time we prepare the ionic-hydrogel electrodes, we soak the hydrogel in 10% NaCl solution long enough for recovery. After about 10 d of storage, the dehydration process becomes irreversible and the contact impedance on forehead reaches above 50 K $\Omega$ . The other method is the one which we adopt eventually in the test. Closed water cycles are formed in the sealed box. Even

after 18 d of storage, the contact impedance on forehead keeps below 10 K $\Omega$ . This simple setup paves the way for real-world BCI applications.

However, there are still some issues that need to be noticed. Firstly, we use a simple multichannel cap with small holes to conduct EEG evaluation. Connecting nut is thus designed to fasten the electrodes on the cap. This structure is not necessary if some other kinds of EEG caps are designed, such as EEG helmet [34]. Secondly, limited by the number of the hydrogel we produce, the long-term performance usability lasts only 18 days. A longer test period and some better storage methods should be explored to assess the long-term hydrogel usability systematically. Furthermore, we should assess the feasibility of the ionic-hydrogel electrodes with more mental tasks and more clinical experiments to expand its potential application fields.

## 5 Conclusion

In this work, soft ionic-hydrogel based electrodes are proposed for EEG signal recording. Unique structures are designed to collect EEG signals according to whether there is hair or not. For EEG measurements on hairy sites, we learn from dry electrodes and design claw-like electrode structures to penetrate the hair. High water contents, softness, and good conductivity of hydrogel are made full use to achieve low skin-electrode impedance. The experimental results show comparable electrical performance and similar EEG signals quality of ionic-hydrogel electrodes with commercial gel electrodes. The results of long-term usability tests, prompt electrodes setup and no residues also show the potential of ionic-hydrogel electrodes for BCI application in daily life.

*This work was supported by the National Key R&D Program of China (Grant No. 2018YFB1307200), the National Natural Science Foundation of China (Grant Nos. 91948302, and 51905339), and the Science and Technology Commission of Shanghai Municipality (Grant No. 18JC1410400).*

- 1 Michel C M, Murray M M. Towards the utilization of EEG as a brain imaging tool. *Neuro Image*, 2012, 61: 371–385
- 2 Iturrate I, Antelis J M, Kubler A, et al. A noninvasive brain-actuated wheelchair based on a P300 neurophysiological protocol and automated navigation. *IEEE Trans Robot*, 2009, 25: 614–627
- 3 Hwang H J, Lim J H, Jung Y J, et al. Development of an SSVEP-based BCI spelling system adopting a QWERTY-style LED keyboard. *J Neuro Sci Methods*, 2012, 208: 59–65
- 4 Meng J, Zhang S, Bekyo A, et al. Noninvasive electroencephalogram based control of a robotic arm for reach and grasp tasks. *Sci Rep*, 2016, 6: 38565
- 5 Ang K K, Chua K S G, Phua K S, et al. A randomized controlled trial of EEG-based motor imagery brain-computer interface robotic rehabilitation for stroke. *Clin EEG Neurosci*, 2015, 46: 310–320
- 6 Alonso-Valerdi L M, Salido-Ruiz R A, Ramirez-Mendoza R A. Motor imagery based brain-computer interfaces: An emerging technology to rehabilitate motor deficits. *Neuropsychologia*, 2015, 79: 354–363

- 7 Al-qaysi Z T, Zaidan B B, Zaidan A A, et al. A review of disability EEG based wheelchair control system: Coherent taxonomy, open challenges and recommendations. *Comput Methods Programs Biomed*, 2018, 164: 221–237
- 8 Li G, Wang S, Duan Y Y. Towards conductive-gel-free electrodes: Understanding the wet electrode, semi-dry electrode and dry electrode-skin interface impedance using electrochemical impedance spectroscopy fitting. *Sens Actuat B-Chem*, 2018, 277: 250–260
- 9 Kaitainen S, Kutvonen A, Suvanto M, et al. Liquid silicone rubber (LSR)-based dry bioelectrodes: The effect of surface micropillar structuring and silver coating on contact impedance. *Sens Actuat A-Phys*, 2014, 206: 22–29
- 10 Son Y J, Worth Longest P, Hindle M. Aerosolization characteristics of dry powder inhaler formulations for the excipient enhanced growth (EEG) application: Effect of spray drying process conditions on aerosol performance. *Int J Pharm*, 2013, 443: 137–145
- 11 Fiedler P, Muhle R, Griebel S, et al. Contact pressure and flexibility of multipin dry EEG electrodes. *IEEE Trans Neural Syst Rehabil Eng*, 2018, 26: 750–757
- 12 Chen Y H, de Beeck M, Vanderheyden L, et al. Soft, comfortable polymer dry electrodes for high quality ECG and EEG recording. *Sensors*, 2014, 14: 23758–23780
- 13 Volosyak I, Valbuena D, Malechka T, et al. Brain-computer interface using water-based electrodes. *J Neural Eng*, 2010, 7: 066007
- 14 Gao K P, Yang H J, Liao L L, et al. A novel bristle-shaped semi-dry electrode with low contact impedance and ease of use features for EEG signal measurements. *IEEE Trans Biomed Eng*, 2020, 67: 750–761
- 15 Mathewson K E, Harrison T J L, Kizuk S A D. High and dry? Comparing active dry EEG electrodes to active and passive wet electrodes. *Psychophysiology*, 2017, 54: 74–82
- 16 Huang S, Liu Y, Zhao Y, et al. Flexible electronics: Stretchable electrodes and their future. *Adv Funct Mater*, 2019, 29: 1805924
- 17 Huang Y A, Dong W, Zhu C, et al. Electromechanical design of self-similar inspired surface electrodes for human-machine interaction. *Complexity*, 2018, 2018: 1–14
- 18 Guiseppi-Elie A. Electroconductive hydrogels: Synthesis, characterization and biomedical applications. *Biomaterials*, 2010, 31: 2701–2716
- 19 Lu B, Yuk H, Lin S, et al. Pure PEDOT:PSS hydrogels. *Nat Commun*, 2019, 10: 1043
- 20 Alba N A, Scelabassi R J, Sun M, et al. Novel hydrogel-based preparation-free EEG electrode. *IEEE Trans Neural Syst Rehabil Eng*, 2010, 18: 415–423
- 21 Lepola P, Myllymaa S, Töyräs J, et al. Screen-printed EEG electrode set for emergency use. *Sens Actuat A-Phys*, 2014, 213: 19–26
- 22 Fernandes M S, Dias N S, Silva A F, et al. Hydrogel-based photonic sensor for a biopotential wearable recording system. *Biosens Bioelectron*, 2010, 26: 80–86
- 23 Pedrosa P, Fiedler P, Schinaia L, et al. Alginate-based hydrogels as an alternative to electrolytic gels for rapid EEG monitoring and easy cleaning procedures. *Sens Actuat B-Chem*, 2017, 247: 273–283
- 24 Gu G, Xu H, Peng S, et al. Integrated soft ionotronic skin with stretchable and transparent hydrogel-elastomer ionic sensors for hand-motion monitoring. *Soft Robotics*, 2019, 6: 368–376
- 25 Romo Vázquez R, Vélez-Pérez H, Ranta R, et al. Blind source separation, wavelet denoising and discriminant analysis for EEG artefacts and noise cancelling. *BioMed Signal Processing Control*, 2012, 7: 389–400
- 26 Li G, Wang S, Duan Y Y. Towards gel-free electrodes: A systematic study of electrode-skin impedance. *Sens Actuat B-Chem*, 2017, 241: 1244–1255
- 27 Park Y G, Choi J, Lee C, et al. Heterogeneity of tremor mechanisms assessed by tremor-related cortical potential in mice. *Mol Brain*, 2015, 8: 3
- 28 Klimesch W. EEG alpha and theta oscillations reflect cognitive and memory performance: A review and analysis. *Brain Res Rev*, 1999, 29: 169–195
- 29 Bin G, Gao X, Yan Z, et al. An online multi-channel SSVEP-based brain-computer interface using a canonical correlation analysis method. *J Neural Eng*, 2009, 6: 046002
- 30 Ferree T C, Luu P, Russell G S, et al. Scalp electrode impedance, infection risk, and EEG data quality. *Clin Neurophysiol*, 2001, 112: 536–544
- 31 Bai Y, Chen B, Xiang F, et al. Transparent hydrogel with enhanced water retention capacity by introducing highly hydratable salt. *Appl Phys Lett*, 2014, 105: 151903
- 32 Löfhede J, Seoane F, Thordstein M. Textile electrodes for EEG recording—A pilot study. *Sensors*, 2012, 12: 16907–16919
- 33 Lopez-Gordo M, Sanchez-Morillo D, Valle F. Dry EEG electrodes. *Sensors*, 2014, 14: 12847–12870
- 34 Von Rosenberg W, Chanwimalueang T, Goverdovsky V, et al. Smart helmet: Wearable multichannel ECG and EEG. *IEEE J Transl Eng Health Med*, 2016, 4: 1–11